

# Raman scattering of electronic surface and bulk states in the giant Rashba, polar semiconductor BiTeI

V. Gnezdilov,<sup>1,2</sup> D. Wulferding,<sup>1</sup> P. Lemmens,<sup>1</sup> A. Möller,<sup>3</sup> P. Recher,<sup>4</sup> H. Berger,<sup>5</sup> R. Sankar,<sup>6</sup> and F. C. Chou<sup>6</sup>

<sup>1</sup>*Institute for Condensed Matter Physics, Technical University of Braunschweig, Mendelssohnstr. 3, D-38106 Braunschweig, Germany*

<sup>2</sup>*B. I. Verkin Institute for Low Temperature Physics and Engineering of the National Academy of Sciences of Ukraine, Kharkov 61103, Ukraine*

<sup>3</sup>*Department of Chemistry and Texas Center for Superconductivity, University Houston, Houston, Texas 77204-5003, United States*

<sup>4</sup>*Institute for Mathematical Physics, Technical University of Braunschweig, Mendelssohnstr. 3, D-38106 Braunschweig, Germany*

<sup>5</sup>*Institute de Physique de la Matière Complexe, EPFL, CH-1015 Lausanne, Switzerland*

<sup>6</sup>*Center for Condensed Matter Sciences, National Taiwan University, Taipei, 10617 Taiwan*  
(Dated: March 20, 2013)

In the giant Rashba, polar semiconductor BiTeI phonons as well as spin split bulk and surface states are probed using Raman scattering. The observed bulk states are in good agreement with symmetry considerations and photoemission data of spin splitting. A very large enhancement of the Raman scattering cross section is observed if the laser energy is tuned to interband transitions. This resonance allows to probe also surface scattering. The respective signal at low energies depends strongly on surface termination and surface potential shifts induced by the cleaving process. The resolved electronic scattering rate is not too different from a corresponding signal of surface states in the topological insulator Bi<sub>2</sub>Se<sub>3</sub>. In the latter materials Rashba split quantum well states are observed that are induced by band bending, leading to a surprising similarity of the two materials.

PACS numbers: 71.20.Nr, 71.70.Ej, 78.30.Am

## I. INTRODUCTION

In the developing field of spintronics, materials are investigated that allow to manipulate and use the electron spin for information processing, e.g. by taking advantage of spin induced energy splittings of electronic states. Three conditions have been identified to lead to such splittings of large magnitude without an external magnetic field:<sup>1</sup> (i) large atomic spin-orbit interaction in an inversion-asymmetric media, (ii) a narrow band gap, and (iii) the presence of highest energy valence and lowest energy conduction bands of the same symmetry. A related aspect is Rashba coupling, based on both the symmetry of the structure and large spin orbit coupling.<sup>2</sup> Rashba coupling leads to a spin polarization depending momentum shift  $k_R$  and a resulting spin splitting of the electronic dispersions.<sup>3</sup> This shift is inevitably connected with broken inversion symmetry. Spin splittings of the order of several meV in zero magnetic fields have been found in InGaAs/InAlAs heterostructures,<sup>4</sup> semiconductor interfaces,<sup>5</sup> and non-magnetic metallic surfaces.<sup>6-8</sup> A much larger splitting of the order of 200 meV has been reported for silver surfaces covered by Bi.<sup>8</sup>

In BiTeI only recently a so called giant Rashba effect has been discovered with a spin splitting of the order of 0.4 eV at the Fermi surface.<sup>9</sup> This compound is a layered, polar semiconductor and crystallizes in the primitive trigonal space group,  $P3m1 = C_{3v}^1$ , No. 156, with one formula unit per unit cell ( $z=1$ ). The crystals structure exhibits trigonal layers of the respective chemical elements with different relative orientation with respect

to their stacking sequence along the crystallographic  $c$ -axis, see Fig. 1. The chemical bonding between Bi and Te can be described as more covalent in character than the Bi-I interaction. Nevertheless, both anions are involved in covalent bonding with Bi and across those void layers ( $\square$ ) exhibit dominant van-der-Waals type interaction. The latter is a much weaker interaction and thus allows two different surfaces, Te- and I-terminated, to be obtained by cleaving. This situation leads to a sufficient electric gradient that could significantly enhance Rashba coupling.<sup>10</sup>

BiTeI is in compliance with all three conditions discussed above.<sup>1,11,12</sup> Photoemission,<sup>9</sup> optical absorption,<sup>13</sup> and Shubnikov-de Haas oscillations<sup>10</sup> have been used to characterize the Rashba-split branches. As function of pressure even a transition into a topologically ordered state has been predicted.<sup>2</sup> Spin-orbit coupling leads to a general softening of phonon frequencies as shown in a combined band structure and Raman scattering investigation of BiTeI and BiTeCl.<sup>14</sup>

Surprisingly, BiTeI has surface electronic states that have a comparably large giant Rashba spin splitting as the bulk states.<sup>11,15</sup> This has an enormous relevance for spintronic applications. These states show a decisive dependence on surface termination while their momentum shift is insensitive to changes of the surface potential.<sup>16,17</sup> If Te terminated the surface leads to occupied surface states as the corresponding bands bend below the bulk valence bands. The opposite happens for I termination.

Spin-orbit coupling is essential for the Rashba splitting in BiTeI. In the topological insulator Bi<sub>2</sub>Se<sub>3</sub> with

an inversion center it can be accounted for surface states with spin momentum locking and topological order.<sup>18–20</sup>  $\text{Bi}_2\text{Se}_3$  is also a small gap ( $\Delta = 0.3$  eV), degenerate semiconductor with a similar doping due to nonstoichiometry. It has a layered, rhombohedral crystal structure ( $D_{3d}^5$ ). For the two compounds the interatomic distances are very similar and the size of the gap in  $\text{Bi}_2\text{Se}_3$  and the spin splitting in  $\text{BiTeI}$  are of similar magnitude. The topological protection of the surface states of  $\text{Bi}_2\text{Se}_3$  involves only elastic backscattering processes. Nevertheless, at present also inelastic scattering processes of the Dirac states are discussed, e.g. based on scanning tunneling spectroscopy<sup>21</sup> and Raman experiments.<sup>22</sup> It is therefore of interest to compare the giant Rashba system  $\text{BiTeI}$  and topological insulators with respect to scattering processes of the surface states. This comparison could shed some light on the role and interplay of spin orbit coupling with other degrees of freedom in these materials.

We have performed Raman scattering experiments on  $\text{BiTeI}$  single crystals and have observed bulk phonon and electronic excitations with a pronounced resonance as function of the incident laser radiation. Low energy excitations that are attribute to surface scattering are observed only on one type of surface, similarly to predictions concerning the electronic properties of certain surface terminations. Furthermore, in Raman scattering these states show a similar phenomenology as the topological surface states in  $\text{Bi}_2\text{Se}_3$ . This is attributed to a comparable quasiparticle dynamics in both classes of materials.

## II. EXPERIMENTAL

Raman scattering experiments in quasi-backscattering geometry using a  $\lambda = 532$  nm solid state laser were performed in single crystals prepared both by transport and Bridgman techniques. The presented data is from crystals from latter technique. Circular light polarizations are denoted by  $RR$  and  $RL$ . To probe resonances of the scattering cross sections we used different laser lines of an argon-krypton mixed ion laser. Due to the low melting point of  $\text{BiTeI}$  ( $520^\circ\text{C}$ ) special care has been taken not to deteriorate the sample surfaces with the incident laser. The laser power was set to 5 mW with a spot diameter of approximately  $100\ \mu\text{m}$  to avoid heating effects. All measurements were carried out in an evacuated closed cycle cryostat in the temperature range from 6.5 K to 295 K. The spectra were collected using a triple Raman spectrometer (Dilor-XY-500) with an attached liquid nitrogen cooled CCD (Horiba Jobin-Yvon, Spectrum One CCD-3000V).

Freshly cleaved sample surfaces were prepared at ambient conditions using scotch tape from the “top” as well as from the “bottom” of large single crystals (typical size  $4 \times 4 \times 2\ \text{mm}^3$ ). Cleaved-off pieces as well as their opposite faces of the single crystals are rapidly cooled down in vacuum to minimize surface degradation. The prepa-

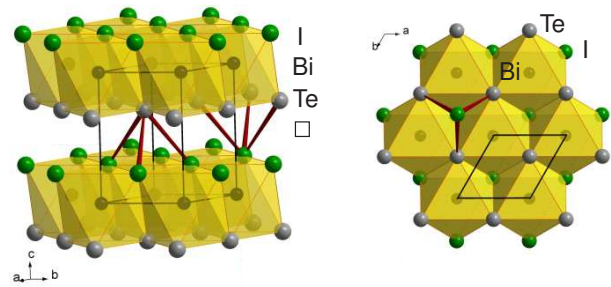


FIG. 1. (Colour online) Sketch of the crystal structure of  $\text{BiTeI}$  in two projections. Layers of Bi, Te, I and voids are marked. Selected bonds that are cut by cleaving and establish the Te and I terminated surface are drawn by thick lines.

ration of cleaved single crystal surfaces of layered  $\text{V}_2\text{VI}_3$  compounds at ambient conditions is known for inducing a surface water layer that later shifts the chemical potential as a function of time. We have therefore carefully checked time dependencies and found evidence that scattering attributed to surface modes is affected by such effects.

## III. RESULTS AND DISCUSSION

### A. Phonon scattering

Low-frequency Raman spectra of  $\text{BiTeI}$  from the  $ab$ -plane in parallel ( $XX$ ) and crossed ( $YX$ ) and two circular polarization configurations are shown in Fig. 2. The spectra are well polarized and four strong lines can be easily identified in the spectra. According to the space group  $P3m1$ , the Bi, Te, and I have site symmetries given by  $1c$ ,  $1b$ , and  $1a$ , respectively. This, indeed, leads to  $\Gamma = 2A_1 + 2E = 4$  Raman-active phonon modes. Lines located at  $93$  and  $150\ \text{cm}^{-1}$  are assigned to  $A_1(1)$  and  $A_1(2)$  phonon modes. The lines at  $55$  and  $102\ \text{cm}^{-1}$  correspond to  $E(1)$  and  $E(2)$  phonon modes, respectively. These phonon lines are superimposed by a structured but weaker background of probably defect or electronic scattering origin (see Fig. 3). With exception of the  $A_1(2)$  mode at  $150\ \text{cm}^{-1}$  all Raman active phonon have a symmetric line shape. We interpret the asymmetric line shape of the latter mode as due to coupling to electronic degrees of freedom (Fano line shape). A similar asymmetry has been observed in optical absorption of a mode at  $143\ \text{cm}^{-1}$ .<sup>23</sup> The spectra from samples grown by Bridgman and transport techniques are identical with respect to the phonon frequencies. Slight deviations exist with respect to the intensity of some phonons and the background scattering. The shown data are in general agreement with an earlier Raman scattering and band structure investigation of  $\text{BiTeI}$  and  $\text{BiTeCl}$ .<sup>14</sup>

In Fig. 3 the temperature evolution of the  $XX$  spectra is shown. Upon warming up to room temperature the phonon modes undergo a moderate softening and their

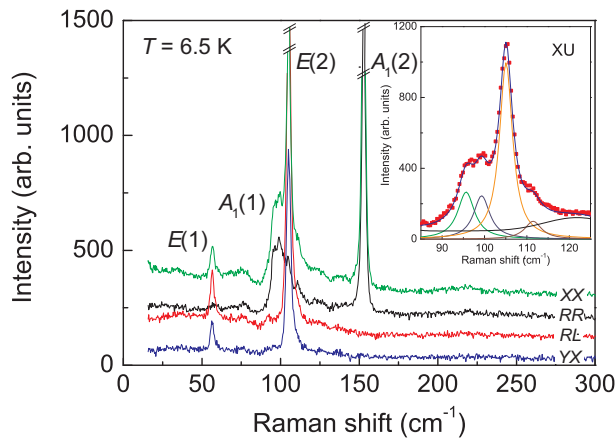


FIG. 2. (Colour online) Polarized Raman spectra in different scattering configurations of the single crystal surface, including circular polarizations of BiTeI at  $T = 6.5$  K and  $\lambda = 532$  nm. Spectra are shifted in intensity for clarity. The phonons with higher scattering intensity are cut off to emphasize signals with smaller intensity. The inset gives a fit by Lorentzian lines to an unpolarized Raman spectrum.

linewidths are increasing. The low temperature data with small linewidths allows a fitting to individual Lorentzian lines, shown in Fig. 2. According to this analysis and general knowledge on light scattering in semiconductors<sup>24</sup> there exists a splitting of the dipole-active lattice vibrations of the order of  $5 \text{ cm}^{-1}$  into doublets of longitudinal (LO) and transverse (TO) vibrations. These doublets are observed as in our experiment the scattering wave vector  $\mathbf{q}$  has a component perpendicular to the crystallographic  $c$  axis. We have omitted a further analysis of these modes as these aspects are not in the center of our investigation and refer to Ref.<sup>14</sup>.

Raman scattering with different incident Laser energies may lead to important information about electronic states involved in the scattering process. Respective data using discrete laser lines in the energy range 1.96 to 2.54 eV lead to a large change of the phonon mode intensity situated in the high photon energy regime. In contrast, we do not observe a general change or increase of the background scattering. This might support its assignment to defect scattering. In Fig 4 resonant Raman profiles determined from three phonon modes are shown. These normalized dependencies overlap very well and we follow a resonant enhancement of the intensity at  $\sim 2.4$  eV ( $T = 6.5$  K). This characteristic energy fits to some electronic dispersions at the  $\Gamma$  point.<sup>1,9</sup> Therefore we attribute the resonance to an interband transition. It is interesting to note that also in the centrosymmetric  $\text{Bi}_2\text{Se}_3$  a resonant enhancement of the scattering intensity has been observed and used to amplify the sensitivity of the experiments.<sup>22</sup>

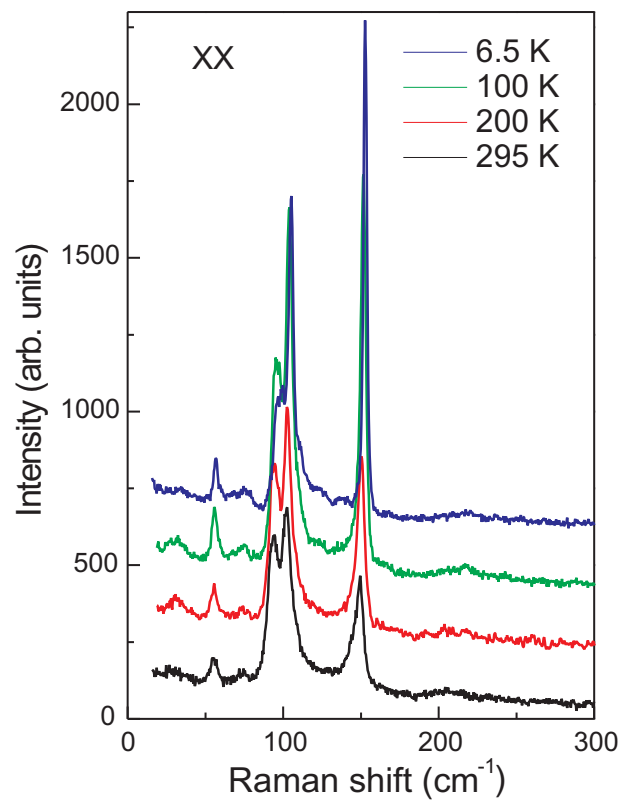


FIG. 3. (Colour online) Temperature evolution of the  $XX$  Raman spectra of BiTeI with  $\lambda = 532$  nm.

## B. Bulk electron scattering

We also searched the high energy spectral range for excitations and found two narrow and weak lines in  $XX$  polarized Raman spectra at about 1550 (0.19 eV) and 2323  $\text{cm}^{-1}$  (0.29 eV), see Fig. 5. The nonobservation of these lines in  $XY$  polarization implies that they are not related to spin-flip or one-magnon scattering but to an electronic scattering process of interband character. Such a process, while weak in intensity is not screened by Coulomb interaction in contrast to intraband electronic fluctuations. In optical reflectivity two intraband transitions from the Fermi level to the conduction bands have been observed, denoted by  $\alpha$  and  $\beta$ , in the inset of Fig. 5. These transitions originate from the Rashba splitting of the electronic bands. The energies of our modes perfectly correspond to the optical and photoemission data and are therefore another independent proof of the giant Rashba splitting in BiTeI. On the other side the small line width of the modes is noteworthy. This evidences a rather small interaction with the continuum of bulk states which they are energetically close to, see inset of Fig. 5.

The intensity of intraband transitions should be proportional to the carrier density  $n$  as they are related to the Fermi surface area. However, only the energy of the intraband transition  $\alpha$  strongly depends on  $n$ , while  $\beta$

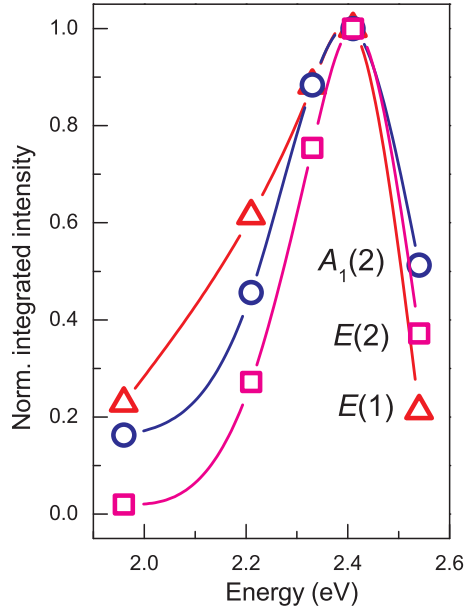


FIG. 4. (Colour online) Normalized resonant intensity profiles for three phonon lines as function of incident Laser energy.

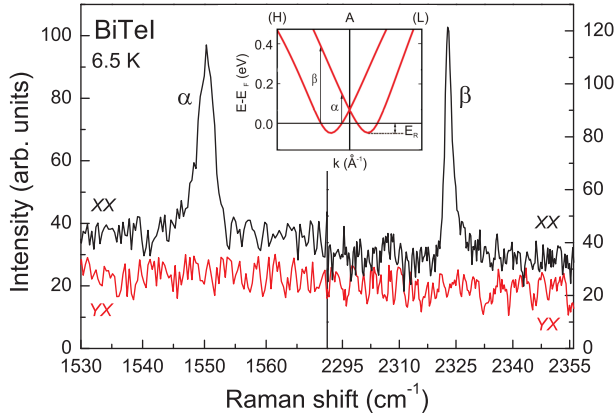


FIG. 5. (Colour online) High frequency Raman spectra of BiTeI measured in  $XX$  and  $YX$  scattering geometries at 6.5 K. The inset shows the band dispersion near the  $A$  point with the spin polarization dependent shifts of the bands. Possible optical transitions are indicated by arrows denoted by  $\alpha$  and  $\beta$ .

is nearly independent, see inset of Fig. 5. This is expected, as with increasing  $n$ , the Fermi level shifts to the band crossing point and, consequently,  $\alpha$  shifts towards zero energy.<sup>13</sup> Based on our observations, we conclude that  $E_F$  of the studied sample is located below the band crossing point. Note also that the light penetration depth of visible light in BiTeI is around 1000 Å which is much larger than the estimated ( $d \sim 20$  Å) thickness of the band-bending surface layer where a significant accumulation of electrons is achieved.<sup>9</sup>

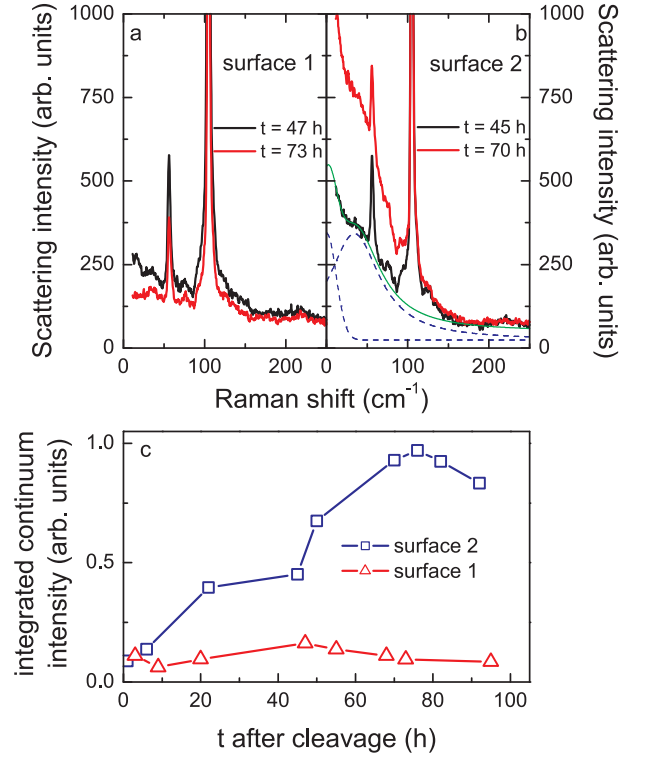


FIG. 6. (Colour online) Raman spectra of BiTeI obtained on a) surface 1 (i.e. the thin, cleaved-off layer) and b) surface 2 (opposite bulk piece). The spectra were measured at  $T = 6.5$  K and in  $RL$  polarization two (black curve) and three (red curve) days after cleaving. c) Time evolution of the low energy continuum for both surfaces over a period of 4 days.

### C. Surface scattering

In the following we will discuss effects that we attribute to electronic surface states of BiTeI. This assignment is based on their spectral range and phenomenology as discussed below. From ARPES experiments as well as theory it is known that BiTeI shows specific electronic surface states that are also spin split.<sup>15,16</sup>

In Fig. 6 we show Raman spectra from two different surface types denoted as surface 1 and 2. They correspond to two freshly prepared, opposite faces that are gained by cleaving a single crystal close to the "top". Similar data are achieved taking the two surfaces by cleaving closer to the bottom of the crystal and exchanging the numbering. According to Fig. 1 these faces correspond to the two preferable surface terminations,  $Te$  and  $I$ , that the large difference in ionicity/covalency of the respective bond to the Bi layer exposes. The well defined difference in low energy Raman scattering through the height of the crystal proves that its orientation with respect to the crystallographic  $c$  axis is maintained and that stacking faults can be safely disregarded.

There is no difference in phonon Raman scattering of the two surfaces as the phonons are bulk excitations. However, surface 2 shows an additional low energy sig-



TABLE I. Scattering rates determined from collision dominated Raman scattering in several compounds.

Compound	$\Gamma$ [ $\text{cm}^{-1}$ ]	Width [ $\text{cm}^{-1}$ ]	Reference
<i>BiTeI</i>	34	75	this work
<i>Bi<sub>2</sub>Se<sub>3</sub></i>	39	80	22
<i>Eu<sub>1-x</sub>Gd<sub>x</sub>O</i>	20-45, f(T)	-	26
<i>Na<sub>x</sub>CoO<sub>2</sub></i> , x=0.78	58	-	25

nal for frequencies below  $\Delta\omega \approx 150 \text{ cm}^{-1}$ , indicated by the solid green line in Fig. 6 b. This scattering can be separated into two contributions, see dashed lines. There exist a Lorentzian (linewidth  $w = 75 \text{ cm}^{-1}$ , energy  $E_{max} = 34 \text{ cm}^{-1}$ ) and quasi-elastic scattering ( $E \approx 0$ ). With respect to selection rules, the Lorentzian has dominant intensity in *RL* and *XX* configuration, similar to the E bulk phonons. The low energy scattering on surface 1 is much weaker and could also be a remaining of the weakly temperature dependent continuum that we described earlier and attributed to defects, see Fig. 3.

Quasi-elastic scattering may be attributed to several kind of fluctuations. In contrast, low energy Lorentzian scattering with a linewidth larger than phonon scattering is usually attributed to collision dominated electronic scattering.<sup>25</sup> Such a scattering contribution is observed if there exist one dominant channel of scattering, e.g. on spin or charge polarons, that prevents the usual screening of electronic intraband scattering.<sup>26</sup> The maximum of the Lorentzian gives a reasonable estimate of the scattering rate of this process,  $\Gamma = E_{max}$ .

The observed scattering rate  $\Gamma = 34 \text{ cm}^{-1}$  in BiTeI is comparable to *Eu<sub>1-x</sub>Gd<sub>x</sub>O* in the proximity to a metal insulator transition<sup>26</sup> and *Na<sub>x</sub>CoO<sub>2</sub>* with spin-state polarons, see Table 1.<sup>25</sup> Finally and importantly it is also very close to observations in the topological insulator *Bi<sub>2</sub>Se<sub>3</sub>*.<sup>22</sup> In this compound a maximum with chiral, *RL* symmetry is observed and attributed to scattering from Dirac to bulk states<sup>22</sup>. Such a scattering process of the topologically protected surface states may be surprising. However, it could be related to the generally small spin lifetime of Dirac states due to their spin-momentum locking<sup>27</sup> and that the prohibited scattering concerns only elastic (back scattering) processes. This means that each scattering process in *Bi<sub>2</sub>Se<sub>3</sub>* that is not prohibited by topological protection involves spin scattering.

In BiTeI the surface electron states are not spin-momentum coupled. However, there are peculiarities based on the combination of the spin splitting with the surface state bending. The enormous spin splitting in the proximity of the Fermi energy leads to two differently spin polarized Fermi surfaces, an inner cylindrical and an outer hexagonally warped one. It has been found that larger in-plane potential gradients, corresponding to the localization of states, lead to a larger out-of-plane  $S_z$  component.<sup>11</sup> This effect together with warping enhanced nesting for one spin polarization. Nesting leads to an enhanced electronic scattering for one spin polarization and this, finally, we take responsible for the observed scat-

tering rates similar to polaronic systems. Please note that the termination of the surface determines the energy of the respective spin polarized Fermi surface. Enhanced quasiparticle dynamics at the Te terminated surface have also been proposed by theory. Rough estimations of the quasiparticle scattering rate lead to the range  $\Gamma \approx 0.5 - 4 \text{ meV}$ , see Fig. 3b) in Ref.<sup>11</sup>. This is in reasonable agreement with our experimental data considering that  $5 \text{ meV} \approx 40 \text{ cm}^{-1}$ .

The Lorentzian scattering intensity also shows a remarkable time dependence, see Fig. 6 c. Its intensity starts to increase about 12 h after the cleavage, increases further until it reaches its maximum after about three days. The latter continuum exhibits no pronounced change with time even 5 days after cleavage. For very long times, at about 100 h after cleavage, the quasi-elastic tail dominates the low energy regime and it becomes difficult to separate it from the Lorentzian. As mentioned above, layered halides and chalcogenides are prone to surface modifications and the generation of a surface water layer after cleaving under ambient conditions. This layer and resulting surface reactions shift the chemical surface potential as a function of time. Electronic surface states react on this shift.

Such effects are well documented in photoemission experiments on the Dirac states in *Bi<sub>2</sub>Se<sub>3</sub>*.<sup>29</sup> Here time dependent shifts of the Dirac states below  $E_F$  have been observed that depend on surface conditions. It has been suggested that, e.g. surface reactions with water create time dependent band bendings.<sup>28</sup> Also K and Rb doping of the surface leads to such effects. As a result quantum well states with strong Rashba splittings are directly observed in photo emission. In our experiments on BiTeI the surface states are already spin split and the potential shift only modifies the warping of the spin polarized Fermi surfaces. Warping and nesting of a Fermi surfaces leads to an anisotropic selection of scattering vectors that enhances collision dominated processes.<sup>30</sup> Thereby the intensity of related Raman scattering processes is modified.<sup>31</sup> In addition recent photoemission experiments evidence that the momentum shift and the spin splitting remain unaltered and intact during the band bending.<sup>17</sup> These observations are important details to enable future applications of these states in spintronics.<sup>15</sup>

#### IV. SUMMARY

In summary, Raman scattering experiments in BiTeI show a pronounced resonance of the bulk phonon as well as high energy electronic excitations. The electronic excitations are due to the giant Rashba splittings of the bands and correspond very well to experimental data from photoemission and optical absorption as well as band structure calculations. Additional low energy excitations are observed that decisively depend on surface termination. These states show a high sensitivity on band bending effects exemplified by a dependence of the scattering inten-

sity of the time after cleavage under ambient condition. The Lorentzian contribution to this scattering is modeled as collision dominated scattering with a scattering rate of  $\Gamma = 34 \text{ cm}^{-1}$ . It points to an enhanced quasiparticle dynamics on BiTeI surfaces, very similar to spectral features observed for Dirac states on the topological in-

sulator  $\text{Bi}_2\text{Se}_3$ .

## ACKNOWLEDGMENTS

We acknowledge important discussions with Ch. Ast and S. Ereemeev. This work was supported by DFG, BIGSM and the NTH School *Contacts in Nanosystems*.

- 
- <sup>1</sup> M. S. Bahramy, R. Arita, and N. Nagaosa, Phys. Rev. B **84**, 041202(R) (2011).
  - <sup>2</sup> M. S. Bahramy, B.-J. Yang, R. Arita, and N. N. Nagaosa, cond-mat/1109.5102v2 (2012).
  - <sup>3</sup> E. I. Rashba, Sov. Phys. Solid State **2**, 1109 (1960).
  - <sup>4</sup> B. Das, D. C. Miller, S. Datta, R. Reifenberger, W. P. Hong, P. K. Bhattacharya, J. Singh, and M. Jaffe, Phys. Rev. B **39**, 1411 (1989).
  - <sup>5</sup> J. Nitta, T. Akazaki, H. Takayanagi, T. Enoki, Phys. Rev. Lett. **78**, 1335 (1997).
  - <sup>6</sup> S. LaShell, B. A. McDougall, and E. Jensen, Phys. Rev. Lett. **77**, 3419 (1996).
  - <sup>7</sup> Yu. M. Koroteev, G. Bihlmayer, J. E. Gayone, E. V. Chulkov, S. Blügel, P. M. Echenique, and Ph. Hofmann, Phys. Rev. Lett. **93**, 046403 (2004).
  - <sup>8</sup> C. R. Ast, J. Henk, A. Ernst, L. Moeschini, M. C. Falub, D. Pacilé, P. Bruno, K. Kern, and M. Grioni, Phys. Rev. Lett. **98**, 186807 (2007).
  - <sup>9</sup> K. Ishizaka, M. S. Bahramy, H. Murakawa, M. Sakano, T. Shimojima, T. Sonobe, K. Koizumi, S. Shin, H. Miyahara, A. Kimura, K. Miyamoto, T. Okuda, H. Namatame, M. Taniguchi, R. Arita, N. Nagaosa, K. Kobayashi, Y. Murakami, R. Kumai, Y. Kaneko, Y. Onose, and Y. Tokura, Nature Mater. **10**, 521 (2011).
  - <sup>10</sup> C. Bell, M. S. Bahramy, H. Murakawa, J. G. Checkelsky, R. Arita, Y. Kaneko, Y. Onose, N. Nagaosa, Y. Tokura, and H. Y. Hwang, SLAC-PUB-15184 (2013).
  - <sup>11</sup> S. V. Ereemeev, I. A. Nechaev, and E. V. Chulkov, JETP Lett. **96**, Issue 7, pp 437 (2012).
  - <sup>12</sup> Z.-Y. Zhu, Y.-C. Cheng and U. Schwingenschlögl, New J. of Phys. **15** (2013) 023010.
  - <sup>13</sup> J. S. Lee, G. A. H. Schober, M. S. Bahramy, H. Murakawa, Y. Onose, R. Arita, N. Nagaosa, and Y. Tokura, Phys. Rev. Lett. **107**, 117401 (2011).
  - <sup>14</sup> I. Yu. Sklyadneva, R. Heid, K.-P. Bohnen, V. Chis, V. A. Volodin, K. A. Kokh, O. E. Tereshchenko, P. M. Echenique, and E. V. Chulkov, Phys. Rev. B **86**, 094302 (2012).
  - <sup>15</sup> S. V. Ereemeev, I. A. Nechaev, Y. M. Koroteev, P. M. Echenique, and E. V. Chulkov, Phys. Rev. Lett. **108**, 246802 (2012).
  - <sup>16</sup> G. Landolt, S. V. Ereemeev, Y. M. Koroteev, B. Slomski, S. Muff, M. Kobayashi, V. N. Strocov, T. Schmitt, Z. S. Aliev, M. B. Babanly, I. R. Amiraslanov, E. V. Chulkov, J. Osterwalder, and J. Hugo Dil, Phys. Rev. Lett. **109**, 116403 (2012).
  - <sup>17</sup> A. Crepaldi, L. Moeschini, G. Auts, C. Tournier-Colletta, S. Moser, N. Virk, H. Berger, Ph. Bugnon, Y. J. Chang, K. Kern, A. Bostwick, E. Rotenberg, O. V. Yazyev, and M. Grioni, Phys. Rev. Lett. **109**, 096803 (2012).
  - <sup>18</sup> H. Zhang, Ch.-X. Liu, X.-L. Qi, X. Dai, Zh. Fang, and Sh.-Ch. Zhang, Nature Phys. **5**, 438 (2009).
  - <sup>19</sup> C. L. Kane, and J. E. Moore, Physics World **24**, 32 (2011).
  - <sup>20</sup> M. Z. Hasan, D. Hsieh, Y. Xia, L. A. Wray, S.-Y. Xu, and C. L. Kane, arXiv:1105.0396 (2011) and references therein.
  - <sup>21</sup> S. Kim, M. Ye, K. Kuroda, Y. Yamada, E. E. Krasovskii, E. V. Chulkov, K. Miyamoto, M. Nakatake, T. Okuda, Y. Ueda, K. Shimada, H. Namatame, M. Taniguchi, and A. Kimura, Phys. Rev. Lett. **107**, 056803 (2011).
  - <sup>22</sup> V. Gnezdilov, Yu. G. Pashkevich, H. Berger, E. Pomjakushina, K. Conder, and P. Lemmens, Phys. Rev. B **84**, 195118 (2011).
  - <sup>23</sup> C. Martin, K. H. Miller, S. Buvaev, H. Berger, X. S. Xu, A. F. Hebard, and D. B. Tanner, Temperature dependent infrared spectroscopy of the Rashba spin-splitting semiconductor BiTeI, cond-mat/1209.1656 (2012).
  - <sup>24</sup> R. Loudon, Adv. Phys. **13**, 423 (1964).
  - <sup>25</sup> P. Lemmens, K.-Y. Choi, V. Gnezdilov, E.Ya. Sherman, D.P. Chen, C.T. Lin, F.C. Chou, and B. Keimer, Phys. Rev. Lett. **96**, 167204 (2006) and references therein.
  - <sup>26</sup> H. Rho, C. S. Snow, S. L. Cooper, Z. Fisk, A. Comment, and J.-Ph. Ansermet, Phys. Rev. Lett. **88**, 127401 (2002).
  - <sup>27</sup> V. E. Sacksteder, S. Kettemann, Q.-Sh. Wu, X. Dai, and Zh. Fang, Phys. Rev. B **85**, 205303 (2012).
  - <sup>28</sup> H. M. Benia, C.-T. Lin, K. Kern, and Ch. R. Ast, Phys. Rev. Lett. **107**, 177602 (2011).
  - <sup>29</sup> Z.-H. Zhu, G. Levy, B. Ludbrook, C. N. Veenstra, J. A. Rosen, R. Comin, D. Wong, P. Dosanjh, A. Ubaldini, P. Syers, N. P. Butch, J. Paglione, I. S. Elfimov, and A. Damascelli, PRL **107**, 186405 (2011).
  - <sup>30</sup> A. Virostek and J. Ruvalds, Phys. Rev. B **45**, 347 (1992).
  - <sup>31</sup> Th. P. Devereaux and R. Hackl, Rev. Mod. Phys. **79**, 175 (2007).